TOKYO AXION HELIOSCOPE EXPERIMENT

Y. INOUE[1,4,a], Y. AKIMOTO[2,b], R. OHTA[2], T. MIZUMOTO[2,c], T. HORIE[2], A. YAMAMOTO[3,4], M. MINOWA[1,4]
(Sumico collaboration)
[1] *International Center for Elementary Particle Physics, The University of Tokyo, 7-3-1 Hongo, Bunkyo-ku, Tokyo 113-0033, Japan*

[2] *Department of Physics, School of Science, The University of Tokyo, 7-3-1 Hongo, Bunkyo-ku, Tokyo 113-0033, Japan*

[3] *High Energy Accelerator Research Organization (KEK), 1-1 Oho, Tsukuba, Ibaraki 305-0801, Japan*

[4] *Research Center for the Early Universe (RESCEU), School of Science, The University of Tokyo, 7-3-1 Hongo, Bunkyo-ku, Tokyo 113-0033, Japan*

The Tokyo axion helioscope experiment aims to detect the solar axions which can be produced in the solar core and are arriving to the Earth. It is equipped with a 2.3m-long 4T superconducting magnet to convert axions into photons, a gas container to hold dispersion-matching medium, a PIN-photodiode-array X-ray detector, and a telescope mount mechanism to track the Sun. In the latest measurement, the axion mass range $m_a = 0.84$–$1.00\,\mathrm{eV}$ was scanned. Analysis set a new limit on the axion-photon coupling constant to be $g_{a\gamma} < 5.6$–$13.4 \times 10^{-10}\mathrm{GeV}^{-1}$ at 95% CL. The latest result and the recent status of this experiment are presented.

1 Introduction

1.1 Axion model

The axion is a hypothetical elementary particle which was introduced to solve the "strong-CP problem" in quantum chromodynamics (QCD).[1] The effective Lagrangian contains a P- and CP violating term originating from the nonperturbative effects of QCD, whose strength is proportional to θ, an angular constant of the vacuum. This term is known to be physical and contributing to the electric dipole moment (EDM) of neutron. Moreover, the phase of the quark mass matrix affects it additively as $\bar{\theta} = \theta + \arg\det\mathcal{M}_q$. Thus, the apparent vanishing of the neutron EDM [2] implies the miraculous cancellation of the two independent physical constants.

Peccei and Quinn proposed a solution which involves the spontaneous breaking of a new global U(1) quasisymmetry, by which $\bar{\theta}$ changes dynamically. Although the postulated symmetry, $\mathrm{U}(1)_{\mathrm{PQ}}$, is a symmetry at the Lagrangian level, it must be explicitly broken by the nonperturbative effects of QCD. When it is spontaneously broken, the associated Nambu-Goldstone

[a] Speaker.
[b] Present address: Graduate School of Medicine, The University of Tokyo
[c] Present address: Cosmic-Ray Group, Department of Physics, Graduate School of Science, Kyoto University

boson field should relax to the potential minimum, where $\bar{\theta} = 0$, i.e., CP is conserved. The excitation about this minimum is called the axion and its mass m_a is related to the symmetry-breaking scale f_a by $m_a = \frac{\sqrt{z}}{1+z}\frac{f_\pi m_\pi}{f_a} = 6 \times 10^{15}[\mathrm{eV}^2]/f_a$. As far as the solution to the strong CP problem is concerned, there are no *a priori* values for f_a or m_a.

One of the universal properties of the axion is its coupling to two photons: [3]

$$\mathcal{L}_{a\gamma\gamma} = -\frac{1}{4} g_{a\gamma} a F^{\mu\nu} \tilde{F}_{\mu\nu} = g_{a\gamma} a \vec{E} \cdot \vec{B}, \tag{1}$$

where $\vec{E}$, $\vec{B}$ and a are the electric, magnetic and axion fields. The axion-photon coupling constant $g_{a\gamma}$ is proportional to m_a as

$$g_{a\gamma} = \frac{\alpha}{2\pi f_a}\left[\frac{E}{N} - \frac{2(4+z)}{3(1+z)}\right] = 1.9 \times 10^{-10}\left(\frac{m_a}{1\,\mathrm{eV}}\right)[E/N - 1.92][\mathrm{GeV}^{-1}], \tag{2}$$

where E/N is a parameter dependent on the specific axion model, eg., $E/N = 0$ in the standard KSVZ model, or $E/N = 8/3$ in the GUT-inspired DFSZ model.

1.2 Experimental searches for axions

Axion phenomenology depends primarily on the unknown m_a. If $m_a \sim 10^{-6}$–$10^{-3}\,\mathrm{eV}$, relic axions from the early universe can be attractive candidates for the cold dark matter (CDM). An elegant technique for detecting axions constituting the dark halo of the Milky Way was developed by Sikivie,[4] by which axions resonantly convert to microwave photons in a tunable high-Q cavity permeated by a strong magnetic field. The Axion Dark Matter Experiment (ADMX) [5] and the CARRACK experiment [6] are presently ongoing along this line.

If m_a is at around 1 eV, the Sun can be a powerful source of axions. The technique for detecting solar axions called "the axion helioscope" was also developed by Sikivie.[4] A pioneering experiment based on this idea was performed by Lazarus *et al.*[7] using a fixed dipole magnet, which was followed by the Tokyo axion helioscope (Sumico) [8,9,10] with a solar tracking superconducting magnet, and later by the CERN Axion Solar Telescope (CAST) [11] using a large decommissioned magnet of the LHC. This technique is described in detail in the next section.

Some other solar axion searches, SOLAX,[12] COSME,[13] DAMA,[14] and CDMS,[15] were making use of crystalline detectors such as germanium or NaI(Tl), where the axion Bragg scattering,[16] or the coherent Primakoff conversion in the periodic lattice of crystals, were exploited.

1.3 Axion helioscope

The detection principle of the axion helioscope is illustrated in Fig. 1. Axions are expected to be produced in the solar core through the Primakoff process. The average energy of the solar axions is 4.2 keV and their differential flux expected at the Earth is approximated by [17,18]

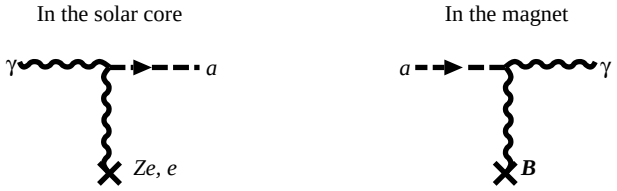

Figure 1: The solar axions produced via the Primakoff process in the solar core are, then, converted into X-rays via the inverse process in the magnet.

$$\begin{aligned} \mathrm{d}\Phi_a/\mathrm{d}E &= 6.020 \times 10^{10}[\mathrm{cm}^{-2}\mathrm{s}^{-1}\mathrm{keV}^{-1}] \\ &\quad \times \left(\frac{g_{a\gamma}}{10^{-10}\mathrm{GeV}^{-1}}\right)^2 \left(\frac{E}{1\,\mathrm{keV}}\right)^{2.481} \exp\left(-\frac{E}{1.205\,\mathrm{keV}}\right), \end{aligned} \tag{3}$$

where E is the energy of the axions. They would be converted into X-ray photons through the inverse process in a strong magnetic field at a laboratory. The conversion rate is given by

$$P_{a\to\gamma} = \frac{g_{a\gamma}^2}{4} \exp\left[-\int_0^L \mathrm{d}z\,\Gamma\right] \times \left|\int_0^L \mathrm{d}z\, B_\perp \exp\left[i\int_0^z \mathrm{d}z'\left(q - \frac{i\Gamma}{2}\right)\right]\right|^2, \tag{4}$$

where z and z' are the coordinate along the incident solar axion, $B_\perp$ is the strength of the transverse magnetic field, L is the length of the field along z-axis, Γ is the X-ray absorption coefficient of the filling medium, $q = k_\gamma - k_a \approx (m_\gamma^2 - m_a^2)/2E$ is the momentum transfer by the virtual photon, and m_γ is the effective mass of the photon in medium.

In vacuum, $m_\gamma = 0$ limiting the sensitive mass range below $m_a \lesssim O(\sqrt{\pi E/L})$ due to the loss of coherence by non-zero q. In a buffer gas, however, coherence can be restored for heavier axions if m_γ could be adjusted to m_a. In light gas such as hydrogen or helium, m_γ is well approximated by $m_\gamma = \sqrt{4\pi\alpha N_e/m_e}$, where α is the fine structure constant, m_e is the electron mass, and N_e is the number density of electrons.

1.4 The Tokyo axion helioscope experiment

The Tokyo axion helioscope or Sumico is an axion helioscope using a dedicated superconducting magnet mounted on a precision solar tracking system. In 1997, Phase 1 measurement [8] was performed without the gas container. From the absence of the expected signals from axions, a limit on axion-photon coupling constant was set to be $g_{a\gamma} < 6.0 \times 10^{-10}\mathrm{GeV}^{-1}$ at 95% CL. The sensitive mass range was limited below $m_a < 0.03\,\mathrm{eV}$ because of the vacuum conversion region. In Phase 2,[9] the apparatus was upgraded to introduce low density ^{4}He gas to the conversion region. The maximum allowed density corresponded to helium gas of 1 atm at the room temperature so that a clogging of the helium pipeline by solid air or moisture would not destroy the cryogenic part of the gas system. The measurement in 2000, together with the Phase 1 result, yielded an upper limit of $g_{a\gamma} < 6.0$–$10.5 \times 10^{-10}\mathrm{GeV}^{-1}$ at 95% CL for $m_a < 0.27\,\mathrm{eV}$. In Phase 3, we are developing an automated, precise, and safe control of higher density cold ^{4}He gas aiming to extend the sensitive mass range up to $m_a \lesssim 2\,\mathrm{eV}$. In the latest measurement in 2007–2008, the mass region $0.84 < m_a < 1.00\,\mathrm{eV}$ was explored. In the following sections, the hardware of the Sumico experiment, result of the latest measurement, and the current status of the experiment are described.

2 Experimental apparatus

The axion helioscope consists of a superconducting magnet, an X-ray detector, a gas container, and an altazimuth mounting to track the Sun. The schematic figure is shown in Fig. 2.

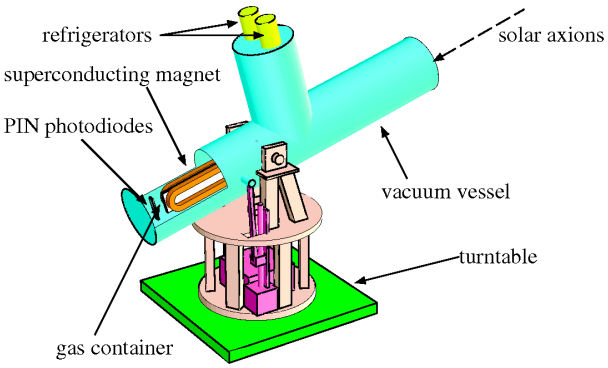

Figure 2: The schematic view of the axion helioscope called the Sumico V detector.

The superconducting magnet [19] consists of two 2.3-m long race-track shaped coils running parallel with a 20-mm wide gap between them. The magnetic field in the gap is 4 T perpendicular to the helioscope axis. The coils are kept at 5–6 K during operation. The magnet is made cryogen-free by two Gifford-McMahon refrigerators cooling directly by conduction, and is equipped with a persistent current switch.

The container to hold buffer gas is inserted in the gap of the magnet. We adopted ^{4}He as the buffer gas, which was kept at $T \lesssim 6\,\mathrm{K}$, just above the critical temperature of ^{4}He, $T_c = 5.2\,\mathrm{K}$. It is worth noting that axions as heavy as a few eV can be reached with helium gas of only about 1 atm and ^{4}He will not liquefy at any pressure at this temperature. The container body is made of four stainless-steel square pipes welded side by side to each other, and is wrapped with 5N high purity aluminium sheet to achieve high uniformity of temperature. The measured thermal conductance between the both ends was $1 \times 10^{-2}\mathrm{W/K}$ at 6 K. The uniformity of the temperature

guarantees the homogeneous density along the length of the container. The detector side of the container is ended with an X-ray window (METOREX C10 custom) which is transparent to X-ray above 2 keV and can withstand up to 0.3 MPa. The container is fixed to the magnet at this side through a temperature-stabilized thermal linkage. The opposite end toward the Sun is blind-ended and is suspended by three Kevlar cords, so that thermal flow through this end is highly suppressed.

To have automatic sequential pressure settings, a gas handling system is built with piezo valves (HORIBASTEC PV1101, PV1302) and a precision pressure gauge (YOKOGAWA MU101-AH1N). For emergency exhaust of the gas in case of rapid temperature increase due to a magnet quenching, a cryogenic rupture disk, which is designed to break at 0.248 MPa, is also introduced into the gas handling system to avoid destruction of the X-ray window by the over pressure.

An array of sixteen PIN photodiodes, Hamamatsu Photonics S3590-06-SPL, is used as the X-ray detector.[20] In the latest measurement, however, twelve of them are used for the analysis because four went defective through thermal stresses. The chip size of a photodiode is $11 \times 11 \times 0.5\,\mathrm{mm}^3$, and the effective area is larger than $9 \times 9\,\mathrm{mm}^2$. It has an inactive surface layer of $\lesssim 0.35\,\mu$m.[21] The output from each photodiode is fed to a charge sensitive preamplifier and waveforms of the preamplifier outputs are digitized using FADCs. We applied off-line pulse shaping to the recorded waveforms.[9] Each photodiode was calibrated by 5.9-keV manganese X-rays from a ^{55}Fe source which is manipulated from the outside and is completely retracted out of the sight of the X-ray detector during the observations.

The entire axion detector is constructed in a vacuum vessel which is mounted on a computer-controlled altazimuth mount. Its trackable altitude ranges from $-28°$ to $+28°$ and its trackable azimuthal range is almost 360°. This range corresponds to an exposure time of about a half of the day in observing the Sun, while background is measured during the rest of the day.

3 Sumico Phase 3 — Measurement, analysis and current status

From December 21 2007 through April 21 2008, a new measurement was performed for 34 gas-density settings with about three days of running time per setting. This time, the azimuthal range was restricted to about 60° because a cable handling system for its unmanned operation is not completed yet. Accordingly, the exposure time was reduced to about a quarter of a day. The scanned mass range was 0.84–1 eV. Since we had not completed the gas relief system, the highest density was determined so that the gas pressure would not exceed the breakage pressure

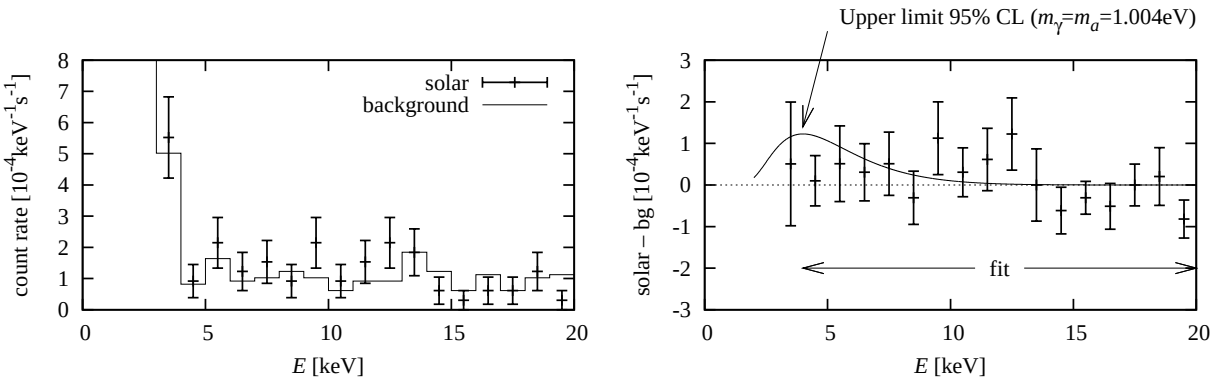

Figure 3: The left figure shows the energy spectrum of the solar observation (error bars) and the background spectrum (solid line) for the effective PIN photodiode area of 371 mm^2 when the gas density was tuned to $m_\gamma = 1.004\,\mathrm{eV}$. The right figure shows the net energy spectrum of the left where the background is subtracted from the solar observation. The solid curve shows the expected solar axion energy spectrum corresponding to the 95% CL upper limit.

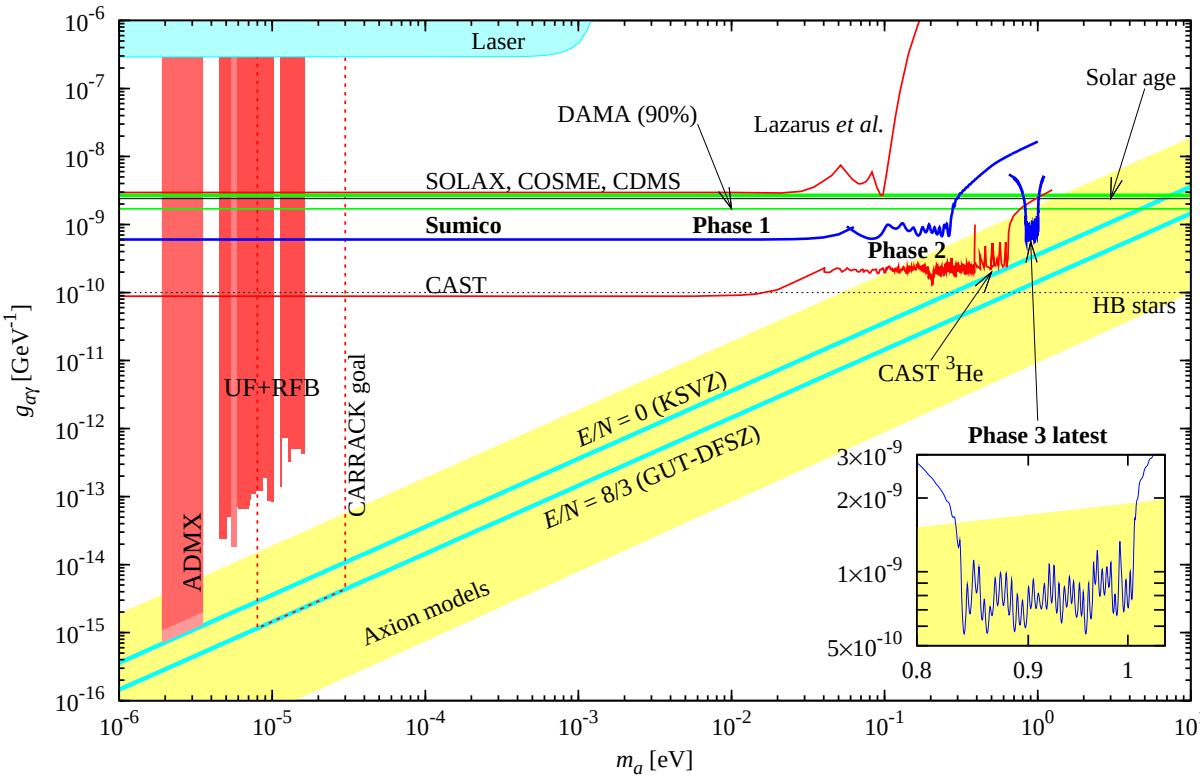

Figure 4: Exclusion plot for $g_{a\gamma}$ as a function of m_a. The yellow band indicates the preferred axion models,[22] in which two slopes (cyan) correspond to two popular models. The new limit [10] by Sumico and the previous ones [8,9] are plotted in blue curves. Other helioscope limits: Lazarus *et al.*[7] and CAST [11] are shown in red curves, axion Bragg scattering experiments: SOLAX,[12] COSME,[13] DAMA,[14] and CDMS [15] are shown in green horizontal lines, two pioneering microwave cavity experiments and ADMX [5] are shown in red area, the newCARRACK prospect is shown in red dashed lines, and Laser based experiments are shown in sky blue area. Two astrophysical bounds considering the solar- (solid black) and HB stars' (dotted black) ages are also shown.

of the rupture disk even during a magnet quenching.

Energy spectra for the solar observation and the background are obtained for each density settings based on the measured direction of the helioscope. Event reduction process was applied in the same way as Phase 2 analysis.[9] In Fig. 3, the energy spectrum of the solar observation with the gas density for $m_\gamma = 1.004\,\mathrm{eV}$ is shown together with the background spectrum as an example. We searched for expected axion signals which scale with $g_{a\gamma}^4$ and vary with m_a in these spectra by applying a series of least-χ^2 fittings. Data from the 34 different gas density settings were combined by using the summed χ^2 of the 34. The energy region of 4–20 keV was used for fitting. No significant excess was seen for any m_a, and thus an upper limit on $g_{a\gamma}$ at 95% CL was given. The smooth curve in Fig. 3 represents an example for the expected axion signal where $m_a = m_\gamma = 1.004\,\mathrm{eV}$ and $g_{a\gamma} = 7.7 \times 10^{-10}\mathrm{GeV}^{-1}$, which corresponds to the upper limit for $m_a = 1.004\,\mathrm{eV}$. Fig. 4 shows the limit plotted as a function of m_a. The previous limits [8,9] and some other bounds (see caption) are also plotted in the same figure.

Currently, upgrades are being continued to deal with cold ^{4}He gas of higher densities. Gas of higher densities requires a higher level of safety against the magnet quenching. The helium pipelines were made thicker for quicker evacuation and the relief valve at the room temperature was replaced based on a new estimation of the maximum flow. A blind-end bellows was attached to the room temperature section of the gas system to prevent the thermoacoustic oscillations which occurred at higher densities. Current effort is being focused on a yet unidentified density-dependent heat influx into the buffer gas.

4 Conclusion

Experimental searches for axions are currently active in two mass regions, where the sensitivities of the experiments have reached the model band. One is at around $m_a \sim 1$–$10\,\mu$eV reached by the cavity dark matter searches. The other is at around $m_a \sim 0.1$–$1\,$eV by the axion helioscopes. Sumico has opened up a new area in the $g_{a\gamma}$-m_a parameter space: $g_{a\gamma} < 6.0$–$10.5 \times 10^{-10}\mathrm{GeV}^{-1}$ (95% CL) for $m_a < 0.27\,$eV and $g_{a\gamma} < 5.6$–$13.4 \times 10^{-10}\mathrm{GeV}^{-1}$ (95% CL) for $m_a = 0.84$–$1.00\,$eV. The latter was the first published helioscope result which scanned in the model band. Although CAST is now leading in terms of the sensitivity owing to its one order of magnitude larger BL value, Sumico is still continuing its development to explore higher masses up to $m_a \lesssim 2\,$eV and is expecting a new measurement this year.

Acknowledgments

The authors thank the former director general of KEK, Professor H. Sugawara, for his support in the beginning of the helioscope experiment. This research was partially supported by the Japanese Ministry of Education, Science, Sports and Culture, Grant-in-Aid for COE Research and Grant-in-Aid for Scientific Research (B), and also by the Matsuo Foundation.

References

1. R. D. Peccei, H. R. Quinn, *Phys. Rev. Lett.* **38**, 1440 (1977); S. Weinberg, *ibid.* **40**, 223 (1978); F. Wilczek, *ibid.* **40**, 279 (1978).
2. C. A. Baker *et al.*, *Phys. Rev. Lett.* **97**, 131801 (2006).
3. D. B. Kaplan, *Nucl. Phys. B* **260**, 215 (1985); M. Srednicki, *ibid.* **260**, 689 (1985).
4. P. Sikivie, *Phys. Rev. Lett.* **51**, 1415 (1983); *ibid.* **52**, 695 (1984) (erratum).
5. S. J. Asztalos *et al.*, *Phys. Rev. Lett.* **104**, 041301 (2010).
6. M. Tada *et al.*, *Nucl. Phys. B (Proc. Suppl.)* **72**, 164 (1999).
7. D. M. Lazarus *et al.*, *Phys. Rev. Lett.* **69**, 2333 (1992).
8. S. Moriyama *et al.*, *Phys. Lett. B* **434**, 147 (1998) [arXiv:hep-ex/9805026].
9. Y. Inoue *et al.*, *Phys. Lett. B* **536**, 18 (2002) [arXiv:astro-ph/0204388].
10. Y. Inoue, *et al.*, *Phys. Lett. B* **668**, 93 (2008) [arXiv:0806.2230].
11. K. Zioutas *et al.*, *Phys. Rev. Lett.* **94**, 121301 (2005); J. Galan, Ph. D thesis, [arXiv:1102.1406].
12. A. O. Gattone *et al.*, *Nucl. Phys. B (Proc. Suppl.)* **70**, 59 (1999).
13. A. Morales *et al.*, *Astropart. Phys.* **16**, 325 (2002).
14. R. Bernabei *et al.*, *Phys. Lett. B* **515**, 6 (2001).
15. Z. Ahmed *et al.*, *Phys. Rev. Lett.* **103**, 141802 (2009).
16. E. A. Paschos, K. Zioutas, *Phys. Lett. B* **323**, 367 (1994).
17. J. N. Bahcall and M. H. Pinsonneault, *Phys. Rev. Lett.* **92**, 121301 (2004).
18. G. G. Raffelt, contribution to *XI International Workshop on "Neutrino Telescope"*, Venice, Italy, 2005.
19. Y. Sato *et al.*, *Development of a Cryogen-free Superconducting Dipole Magnet*, in proceedings of *the 15th International Conference on Magnet Technology (MT-15)*, Science Press, Beijing, 1998, pp. 262–265; KEK-Preprint-97-202 (November, 1997).
20. T. Namba *et al.*, *Nucl. Instr. Meth. A* **489**, 224 (2002) [arXiv:astro-ph/0109041].
21. Y. Akimoto *et al.*, *Nucl. Instr. Meth. A* **557**, 684 (2006) [arXiv:physics/0504147].
22. S. L. Cheng, C. Q. Geng, W.-T. Ni, *Phys. Rev. D* **52**, 3132 (1995).